An introduction to Hybrid High-Order methods

Daniele A. Di Pietro

Institut Montpelliérain Alexander Grothendieck, University of Montpellier

Toulouse, 9 February 2018

Outline

Outline

Features

- Capability of handling general polyhedral meshes
- Construction valid for arbitrary space dimensions
- Arbitrary approximation order (including $k = 0$)
- Robustness with respect to the variations of the physical coefficients
- Reduced computational cost after static condensation

$$N_{\mathrm{dof},h} = \mathrm{card}(\mathcal{F}_h^{\mathrm{i}})\binom{k+d-1}{d-1}$$

Polyhedral meshes

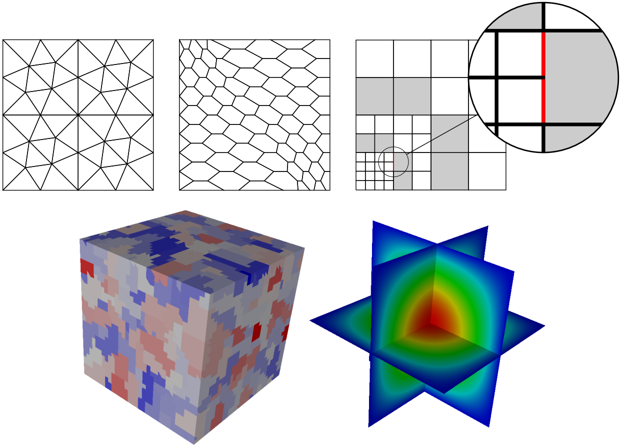

Figure: Admissible meshes in 2d and 3d, and HHO solution on the agglomerated 3d mesh

Model problem

- Let $\Omega \subset \mathbb{R}^d$, $d \geq 1$, denote a bounded, connected polyhedral domain
- For $f \in L^2(\Omega)$, we consider the Poisson problem

$$\begin{aligned} -\triangle u &= f \qquad && \text{in } \Omega \\ u &= 0 \qquad && \text{on } \partial\Omega \end{aligned}$$

- In weak form: Find $u \in H_0^1(\Omega)$ s.t.

$$a(u, v) := (\nabla u, \nabla v) = (f, v) \qquad \forall v \in H_0^1(\Omega)$$

Projectors on local polynomial spaces

- At the core of HHO are projectors on local polynomial spaces
- With $X = T$ or $X = F$, the L^2-projector $\pi_X^{0,l} : L^1(X) \to \mathbb{P}^l(X)$ is s.t.

$$(\pi_X^{0,l} v - v, w)_X = 0 \text{ for all } w \in \mathbb{P}^l(X)$$

- The elliptic projector $\pi_T^{1,l} : W^{1,1}(T) \to \mathbb{P}^l(T)$ is s.t.

$$(\nabla(\pi_T^{1,l} v - v), \nabla w)_T = 0 \text{ for all } w \in \mathbb{P}^l(T) \text{ and } (\pi_T^{1,l} v - v, 1)_T = 0$$

- Both $\pi_T^{0,l}$ and $\pi_T^{1,l}$ have optimal approximation properties in $\mathbb{P}^l(T)$
- See [DP and Droniou, 2017a, DP and Droniou, 2017b]

Computing $\pi_T^{1,k+1}$ from L^2-projections of degree k

- The following integration by parts formula is valid for all $w \in C^\infty(\overline{T})$:

$$\boxed{(\boldsymbol{\nabla} v, \boldsymbol{\nabla} w)_T = -(v, \triangle w)_T + \sum_{F \in \mathcal{F}_T} (v, \boldsymbol{\nabla} w \cdot \boldsymbol{n}_{TF})_F}$$

- Specializing it to $w \in \mathbb{P}^{k+1}(T)$, we can write

$$(\boldsymbol{\nabla} \pi_T^{1,k+1} v, \boldsymbol{\nabla} w)_T = -(\pi_T^{0,k} v, \triangle w)_T + \sum_{F \in \mathcal{F}_T} (\pi_F^{0,k} v_{|F}, \boldsymbol{\nabla} w \cdot \boldsymbol{n}_{TF})_F$$

- Moreover, it can be easily seen that

$$(\pi_T^{1,k+1} v - v, 1)_T = (\pi_T^{1,k+1} v - \pi_T^{0,k} v, 1)_T = 0$$

- **Hence, $\pi_T^{1,k+1} v$ can be computed from $\pi_T^{0,k} v$ and $(\pi_F^{0,k} v_{|F})_{F \in \mathcal{F}_T}$!**

Discrete unknowns

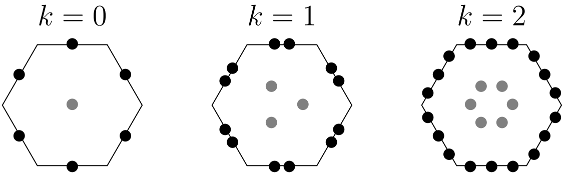

Figure: $\underline{U}_T^k$ for $k \in \{0, 1, 2\}$

- Let a polynomial degree $k \geq 0$ be fixed
- For all $T \in \mathcal{T}_h$, we define the local space of discrete unknowns

$$\underline{U}_T^k := \left\{ \underline{v}_T = (v_T, (v_F)_{F \in \mathcal{F}_T}) \;:\; v_T \in \mathbb{P}^k(T) \text{ and } v_F \in \mathbb{P}^k(F) \quad \forall F \in \mathcal{F}_T \right\}$$

- The local interpolator $\underline{I}_T^k : H^1(T) \to \underline{U}_T^k$ is s.t., for all $v \in H^1(T)$,

$$\underline{I}_T^k v := (\pi_T^{0,k} v, (\pi_F^{0,k} v_{|F})_{F \in \mathcal{F}_T})$$

Local potential reconstruction

- Let $T \in \mathcal{T}_h$. We define the local potential reconstruction operator

$$r_T^{k+1} : \underline{U}_T^k \to \mathbb{P}^{k+1}(T)$$

s.t. for all $\underline{v}_T \in \underline{U}_T^k$, $(r_T^{k+1}\underline{v}_T - v_T, 1)_T = 0$ and

$$\boxed{(\boldsymbol{\nabla} r_T^{k+1}\underline{v}_T, \boldsymbol{\nabla} w)_T = -(v_T, \triangle w)_T + \sum_{F \in \mathcal{F}_T} (v_F, \boldsymbol{\nabla} w \cdot \boldsymbol{n}_{TF})_F \quad \forall w \in \mathbb{P}^{k+1}(T)}$$

- By construction, we have

$$\boxed{r_T^{k+1} \circ \underline{I}_T^k = \pi_T^{1,k+1}}$$

- $r_T^{k+1} \circ \underline{I}_T^k$ has therefore optimal approximation properties in $\mathbb{P}^{k+1}(T)$

Stabilization I

- We would be tempted to approximate

$$a_{|T}(u,v) \approx (\boldsymbol{\nabla} r_T^{k+1}\underline{u}_T, \boldsymbol{\nabla} r_T^{k+1}\underline{v}_T)_T$$

- This choice, however, is not stable in general. We consider instead

$$\boxed{\mathrm{a}_T(\underline{u}_T,\underline{v}_T) := (\boldsymbol{\nabla} r_T^{k+1}\underline{u}_T, \boldsymbol{\nabla} r_T^{k+1}\underline{v}_T)_T + \mathrm{s}_T(\underline{u}_T,\underline{v}_T)}$$

- The role of s_T is to ensure $\|\cdot\|_{1,T}$-coercivity with

$$\|\underline{v}_T\|_{1,T}^2 := \|\boldsymbol{\nabla} v_T\|_T^2 + \sum_{F\in\mathcal{F}_T}\frac{1}{h_F}\|v_F - v_T\|_F^2 \quad \forall \underline{v}_T \in \underline{U}_T^k$$

Stabilization II

Assumption (Stabilization bilinear form)

The bilinear form $\mathrm{s}_T : \underline{U}_T^k \times \underline{U}_T^k \to \mathbb{R}$ satisfies the following properties:

- Symmetry and positivity. s_T is symmetric and positive semidefinite.
- Stability. It holds, with hidden constant independent of h and T,

$$\mathrm{a}_T(\underline{v}_T, \underline{v}_T)^{\frac{1}{2}} \simeq \|\underline{v}_T\|_{1,T} \quad \forall \underline{v}_T \in \underline{U}_T^k.$$

- Polynomial consistency. For all $w \in \mathbb{P}^{k+1}(T)$ and all $\underline{v}_T \in \underline{U}_T^k$,

$$\mathrm{s}_T(\underline{I}_T^k w, \underline{v}_T) = 0.$$

Stabilization III

- The following stable choice violates polynomial consistency:

$$\mathrm{s}_T^{\mathrm{hdg}}(\underline{u}_T, \underline{v}_T) \coloneqq \sum_{F \in \mathcal{F}_T} h_F^{-1}(u_F - u_T, v_F - v_T)_F$$

- To circumvent this problem, we penalize the high-order differences s.t.

$$(\delta_T^k \underline{v}_T, (\delta_{TF}^k \underline{v}_T)_{F \in \mathcal{F}_T}) \coloneqq \underline{I}_T^k r_T^{k+1} \underline{v}_T - \underline{v}_T$$

- The classical HHO stabilization bilinear form reads

$$\boxed{\mathrm{s}_T(\underline{u}_T, \underline{v}_T) \coloneqq \sum_{F \in \mathcal{F}_T} h_F^{-1}((\delta_T^k - \delta_{TF}^k)\underline{u}_T, (\delta_T^k - \delta_{TF}^k)\underline{v}_T)_F}$$

Discrete problem

- Define the global space with single-valued interface unknowns

$$\underline{U}_h^k := \Big\{ \underline{v}_h = ((v_T)_{T\in\mathcal{T}_h}, (v_F)_{F\in\mathcal{F}_h}) \ : \\ v_T \in \mathbb{P}^k(T) \quad \forall T\in\mathcal{T}_h \text{ and } v_F \in \mathbb{P}^k(F) \quad \forall F \in \mathcal{F}_h \Big\}$$

and its subspace with strongly enforced boundary conditions

$$\underline{U}_{h,0}^k := \left\{ \underline{v}_h \in \underline{U}_h^k \ : \ v_F \equiv 0 \quad \forall F \in \mathcal{F}_h^{\mathrm{b}} \right\}$$

- The discrete problem reads: Find $\underline{u}_h \in \underline{U}_{h,0}^k$ s.t.

$$\boxed{\mathrm{a}_h(\underline{u}_h, \underline{v}_h) := \sum_{T\in\mathcal{T}_h} \mathrm{a}_T(\underline{u}_T, \underline{v}_T) = \sum_{T\in\mathcal{T}_h} (f, v_T)_T \quad \forall \underline{v}_h \in \underline{U}_{h,0}^k}$$

- Well-posedness follows from coercivity and discrete Poincaré

Convergence

Theorem (Energy-norm error estimate)

Assume $u \in H_0^1(\Omega) \cap H^{k+2}(\mathcal{T}_h)$. We have the following energy error estimate:

$$\boxed{\|\nabla_h(r_h^{k+1}\underline{u}_h - u)\| + |\underline{u}_h|_{s,h} \lesssim h^{k+1}|u|_{H^{k+2}(\mathcal{T}_h)},}$$

with $(r_h^{k+1}\underline{u}_h)_{|T} := r_T^{k+1}\underline{u}_T$ for all $T \in \mathcal{T}_h$ and $|\underline{u}_h|_{s,h}^2 := \sum_{T\in\mathcal{T}_h} \mathrm{s}_T(\underline{u}_T, \underline{u}_T)$.

Theorem (Superclose L^2-norm error estimate)

Further assuming elliptic regularity and $f \in H^1(\mathcal{T}_h)$ if $k = 0$,

$$\boxed{\|r_h^{k+1}\underline{u}_h - u\| \lesssim h^{k+2}\mathcal{N}_k,}$$

with $\mathcal{N}_0 := \|f\|_{H^1(\mathcal{T}_h)}$ and $\mathcal{N}_k := |u|_{H^{k+2}(\mathcal{T}_h)}$ for $k \geq 1$.

Static condensation I

- Fix a basis for $\underline{U}_{h,0}^k$ with functions supported by only one T or F
- Partition the discrete unknowns into element- and interface-based:

$$\mathsf{U}_h = \begin{bmatrix} \mathsf{U}_{\mathcal{T}_h} \\ \mathsf{U}_{\mathcal{F}_h^{\mathrm{i}}} \end{bmatrix}$$

- U_h solves the following linear system:

$$\begin{bmatrix} \mathsf{A}_{\mathcal{T}_h \mathcal{T}_h} & \mathsf{A}_{\mathcal{T}_h \mathcal{F}_h^{\mathrm{i}}} \\ \mathsf{A}_{\mathcal{F}_h^{\mathrm{i}} \mathcal{T}_h} & \mathsf{A}_{\mathcal{F}_h^{\mathrm{i}} \mathcal{F}_h^{\mathrm{i}}} \end{bmatrix} \begin{bmatrix} \mathsf{U}_{\mathcal{T}_h} \\ \mathsf{U}_{\mathcal{F}_h^{\mathrm{i}}} \end{bmatrix} = \begin{bmatrix} \mathsf{F}_{\mathcal{T}_h} \\ 0 \end{bmatrix}$$

- $\mathsf{A}_{\mathcal{T}_h \mathcal{T}_h}$ **is block-diagonal and SPD, hence inexpensive to invert**

Static condensation II

This remark suggests a two-step solution strategy:

- Element unknowns are eliminated solving the local balances

$$\mathsf{U}_{\mathcal{T}_h} = \mathsf{A}_{\mathcal{T}_h\mathcal{T}_h}^{-1}\left(\mathsf{F}_{\mathcal{T}_h} - \mathsf{A}_{\mathcal{T}_h\mathcal{F}_h^{\mathrm{i}}}\mathsf{U}_{\mathcal{F}_h^{\mathrm{i}}}\right)$$

- Face unknowns are obtained solving the global transmission problem

$$\mathsf{A}_h^{\mathrm{sc}}\mathsf{U}_{\mathcal{F}_h^{\mathrm{i}}} = -\mathsf{A}_{\mathcal{T}_h\mathcal{F}_h}^{\mathrm{T}}\mathsf{A}_{\mathcal{T}_h\mathcal{T}_h}^{-1}\mathsf{F}_{\mathcal{T}_h}$$

  with global system matrix

$$\mathsf{A}_h^{\mathrm{sc}} := \mathsf{A}_{\mathcal{F}_h\mathcal{F}_h} - \mathsf{A}_{\mathcal{T}_h\mathcal{F}_h}^{\mathrm{T}}\mathsf{A}_{\mathcal{T}_h\mathcal{T}_h}^{-1}\mathsf{A}_{\mathcal{T}_h\mathcal{F}_h}$$

$\mathsf{A}_h^{\mathrm{sc}}$ **is SPD and its stencil involves neighbours through faces**

Numerical examples

2d test case, smooth solution, uniform refinement

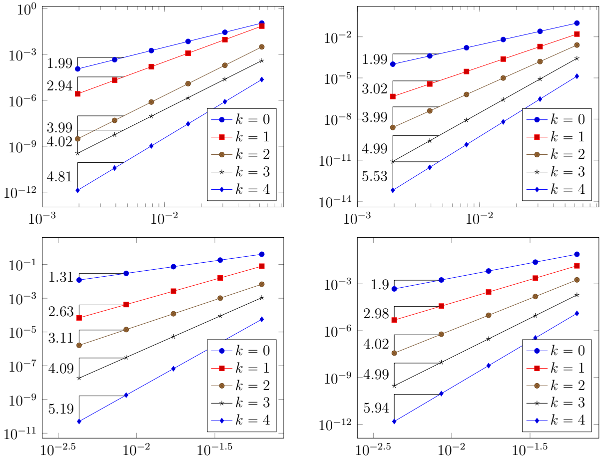

Figure: 2d test case, trigonometric solution. Energy (left) and L^2-norm (right) of the error vs. h for uniformly refined triangular (top) and hexagonal (bottom) mesh families

Numerical examples I

3d industrial test case, adaptive refinement, cost assessment

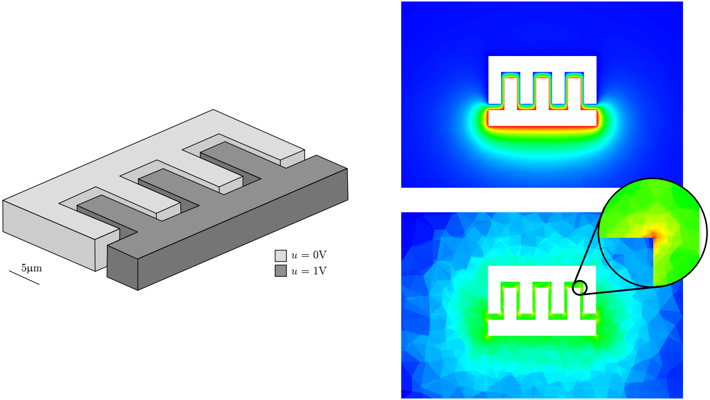

Figure: Geometry (left), numerical solution (right, top) and final adaptive mesh (right, bottom) for the comb-drive actuator test case [DP and Specogna, 2016]

Numerical examples II

3d industrial test case, adaptive refinement, cost assessment

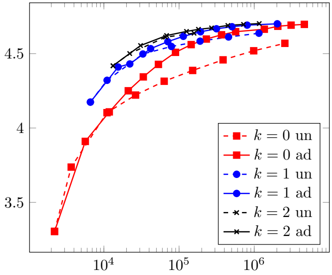

(a) Capacitance vs. $N_{\mathrm{dof},h}$

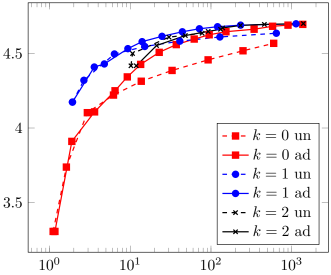

(b) Capacitance vs. computing time

Figure: Results for the comb drive benchmark.

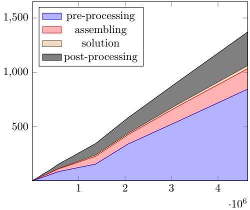

(a) $k = 0$

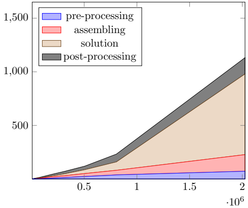

(b) $k = 1$

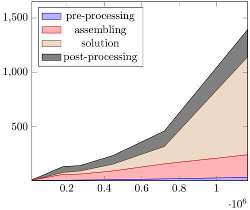

(c) $k = 2$

Figure: Computing wall time (s) vs. number of DOFs for the comb drive benchmark, AGMG solver.

Numerical examples I
3d test case, singular solution, adaptive coarsening

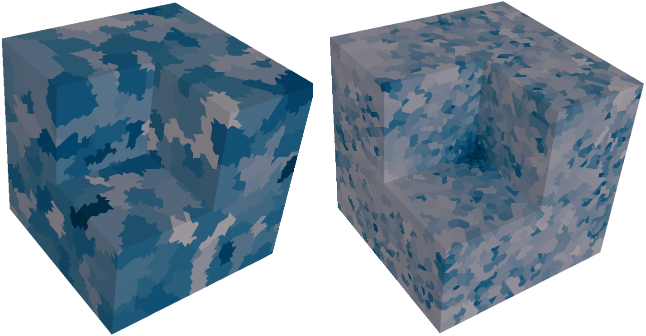

Figure: Fichera corner benchmark, adaptive mesh coarsening [DP and Specogna, 2016]

Numerical examples II

3d test case, singular solution, adaptive coarsening

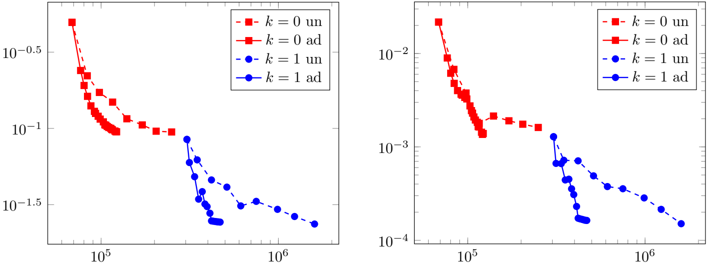

(a) Energy-error vs. N_{dofs}

(b) L^2-error vs. N_{ndof}

Figure: Error vs. number of DOFs for the Fichera corner benchmark, adaptively coarsened meshes

Outline

Features

- Capability of handling general polyhedral meshes
- Construction valid for both $d = 2$ and $d = 3$
- Arbitrary approximation order (including $k = 0$)
- Inf-sup stability on general meshes
- Robust handling of dominant advection
- Reduced computational cost after static condensation

$$N_{\mathrm{dof},h} = d\,\mathrm{card}(\mathcal{F}_h^{\mathrm{i}})\binom{k+d-1}{d-1} + \binom{k+d}{d}$$

A few references

- MHO for Stokes [Aghili, Boyaval, DP, 2015]
- Pressure-robust HHO for Stokes [DP, Ern, Linke, Schieweck, 2016]
- HHO for Navier–Stokes [DP and Krell, 2017]
- Péclet-robust HHO for Oseen [Aghili and DP, 2017]
- Darcy-robust HHO for Brinkman [Botti, DP, Droniou, 2018]

The incompressible Navier–Stokes equations I

- Let $d \in \{2,3\}$, $\nu \in \mathbb{R}_+^*$, $\boldsymbol{f} \in L^2(\Omega)^d$, $\boldsymbol{U} := H_0^1(\Omega)^d$, and $P := L_0^2(\Omega)$
- The INS problem reads: Find $(\boldsymbol{u}, p) \in \boldsymbol{U} \times P$ s.t.

$$\begin{aligned} \nu a(\boldsymbol{u}, \boldsymbol{v}) + t(\boldsymbol{u}, \boldsymbol{u}, \boldsymbol{v}) + b(\boldsymbol{v}, p) &= \int_\Omega \boldsymbol{f} \cdot \boldsymbol{v} \qquad && \forall \boldsymbol{v} \in \boldsymbol{U}, \\ -b(\boldsymbol{u}, q) &= 0 && \forall q \in P, \end{aligned}$$

where

$$a(\boldsymbol{u}, \boldsymbol{v}) := \int_\Omega \boldsymbol{\nabla} \boldsymbol{u} : \boldsymbol{\nabla} \boldsymbol{v}, \quad b(\boldsymbol{v}, q) := -\int_\Omega (\boldsymbol{\nabla} \cdot \boldsymbol{v}) q, \quad t(\boldsymbol{w}, \boldsymbol{u}, \boldsymbol{v}) := \int_\Omega \boldsymbol{v}^{\mathrm{T}} \boldsymbol{\nabla} \boldsymbol{u}\, \boldsymbol{w}$$

- Here, we have used the matrix-product notation, so that

$$\boldsymbol{\nabla} \boldsymbol{u}\, \boldsymbol{u} = \sum_{j=1}^{d} u_j \partial_j \boldsymbol{u}$$

The incompressible Navier–Stokes equations II

- Integrating by parts and using $\boldsymbol{u} = \boldsymbol{0}$ on $\partial\Omega$ and $\boldsymbol{\nabla}\cdot\boldsymbol{w} = 0$ in Ω, we get

$$\boxed{t(\boldsymbol{w}, \boldsymbol{u}, \boldsymbol{v}) = \frac{1}{2}\int_\Omega \boldsymbol{v}^{\mathrm{T}}\boldsymbol{\nabla}\boldsymbol{u}\,\boldsymbol{w} - \frac{1}{2}\int_\Omega \boldsymbol{u}^{\mathrm{T}}\boldsymbol{\nabla}\boldsymbol{v}\,\boldsymbol{w}}$$

- This shows that t is non dissipative: For all $\boldsymbol{w}, \boldsymbol{v} \in \boldsymbol{U}$ it holds

$$t(\boldsymbol{w}, \boldsymbol{v}, \boldsymbol{v}) = 0$$

Discrete spaces I

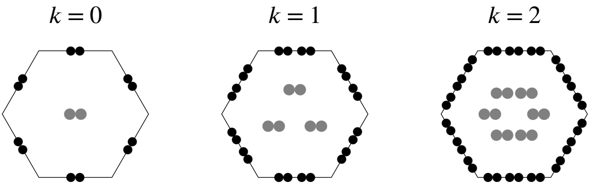

Figure: Local velocity space $\underline{\boldsymbol{U}}_T^k$ for $k \in \{0, 1, 2\}$

- For $k \geq 0$, we define the global space of discrete unknowns

$$\underline{\boldsymbol{U}}_h^k := \Big\{ \underline{\boldsymbol{v}}_h = ((\boldsymbol{v}_T)_{T \in \mathcal{T}_h}, (\boldsymbol{v}_F)_{F \in \mathcal{F}_h}) \;:\; \boldsymbol{v}_T \in \mathbb{P}^k(T)^d \quad \forall T \in \mathcal{T}_h \text{ and } \boldsymbol{v}_F \in \mathbb{P}^k(F)^d \quad \forall F \in \mathcal{F}_h \Big\}$$

- The restriction to $T \in \mathcal{T}_h$ is denoted by $\underline{\boldsymbol{U}}_T^k$, and $\underline{\boldsymbol{v}}_T = (\boldsymbol{v}_T, (\boldsymbol{v}_F)_{F \in \mathcal{F}_T})$

Discrete spaces II

- The global interpolator $\underline{\boldsymbol{I}}_h^k : H^1(\Omega)^d \to \underline{\boldsymbol{U}}_h^k$ is s.t. $\forall \boldsymbol{v} \in H^1(\Omega)^d$

$$\underline{\boldsymbol{I}}_h^k \boldsymbol{v} := ((\boldsymbol{\pi}_T^{0,k} \boldsymbol{v}_{|T})_{T \in \mathcal{T}_h}, (\boldsymbol{\pi}_F^{0,k} \boldsymbol{v}_{|F})_{F \in \mathcal{F}_h})$$

- The velocity space strongly accounting for boundary conditions is

$$\underline{\boldsymbol{U}}_{h,0}^k := \left\{ \underline{\boldsymbol{v}}_h \in \underline{\boldsymbol{U}}_h^k \;:\; \boldsymbol{v}_F = \boldsymbol{0} \quad \forall F \in \mathcal{F}_h^{\mathrm{b}} \right\}$$

- The discrete pressure space is defined setting

$$P_h^k := \left\{ q_h \in \mathbb{P}^k(\mathcal{T}_h) \;\middle|\; \int_\Omega q_h = 0 \right\}$$

Reconstructions of differential operators

- For $l \geq 0$, the gradient reconstruction $\boldsymbol{G}_T^l : \underline{\boldsymbol{U}}_T^k \to \mathbb{P}^l(T)^{d\times d}$ is s.t.

$$\boxed{\int_T \boldsymbol{G}_T^l \underline{\boldsymbol{v}}_T : \boldsymbol{\tau} = -\int_T \boldsymbol{v}_T \cdot (\boldsymbol{\nabla} \cdot \boldsymbol{\tau}) + \sum_{F \in \mathcal{F}_T} \int_F \boldsymbol{v}_F \cdot (\boldsymbol{\tau}\, \boldsymbol{n}_{TF}) \quad \forall \boldsymbol{\tau} \in \mathbb{P}^l(T)^{d\times d}}$$

- The velocity reconstruction $\boldsymbol{r}_T^{k+1} : \underline{\boldsymbol{U}}_T^k \to \mathbb{P}^{k+1}(T)^d$ is s.t.

$$\int_T (\boldsymbol{\nabla} \boldsymbol{r}_T^{k+1} \underline{\boldsymbol{v}}_T - \boldsymbol{G}_T^k \underline{\boldsymbol{v}}_T) : \boldsymbol{\nabla} \boldsymbol{w} = 0 \quad \forall \boldsymbol{w} \in \mathbb{P}^{k+1}(T)^d, \qquad \int_T \boldsymbol{r}_T^{k+1} \underline{\boldsymbol{v}}_T - \boldsymbol{v}_T = \boldsymbol{0}$$

- Global reconstructions are defined setting for all $T \in \mathcal{T}_h$ and $\underline{\boldsymbol{v}}_h \in \underline{\boldsymbol{U}}_h^k$

$$(\boldsymbol{G}_h^l \underline{\boldsymbol{v}}_h)_{|T} \coloneqq \boldsymbol{G}_T^l \underline{\boldsymbol{v}}_T, \quad (\boldsymbol{r}_h^{k+1} \underline{\boldsymbol{v}}_h)_{|T} \coloneqq \boldsymbol{r}_T^{k+1} \underline{\boldsymbol{v}}_T, \quad D_h^k \underline{\boldsymbol{v}}_h \coloneqq \mathrm{tr}(\boldsymbol{G}_h^k \underline{\boldsymbol{v}}_h)$$

Viscous term

- The viscous term is discretized by means of the bilinear form a_h s.t.

$$\mathrm{a}_h(\underline{\boldsymbol{u}}_h, \underline{\boldsymbol{v}}_h) \coloneqq \int_\Omega \boldsymbol{G}_h^k \underline{\boldsymbol{u}}_h : \boldsymbol{G}_h^k \underline{\boldsymbol{v}}_h + \mathrm{s}_h(\underline{\boldsymbol{u}}_h, \underline{\boldsymbol{v}}_h)$$

- As in the scalar case, several possible choices for s_h ensure that

$$C_a^{-1} \|\underline{\boldsymbol{v}}_h\|_{1,h}^2 \leq \mathrm{a}_h(\underline{\boldsymbol{v}}_h, \underline{\boldsymbol{v}}_h) \leq C_a \|\underline{\boldsymbol{v}}_h\|_{1,h}^2 \quad \forall \underline{\boldsymbol{v}}_h \in \underline{\boldsymbol{U}}_h^k$$

  with real number C_a independent of h and of the problem data
- Variable viscosity can be treated following [DP and Ern, 2015]

Pressure-velocity coupling

- The pressure-velocity coupling is realized by means of the bilinear

$$\mathrm{b}_h(\underline{\boldsymbol{v}}_h, q_h) := -\int_\Omega D_h^k \underline{\boldsymbol{v}}_h q_h$$

- A crucial point is that b_h satisfies the following inf-sup condition

$$\boxed{\forall q_h \in P_h^k, \quad \beta \|q_h\|_{L^2(\Omega)} \leq \sup_{\underline{\boldsymbol{v}}_h \in \underline{\boldsymbol{U}}_{h,0}^k, \|\underline{\boldsymbol{v}}_h\|_{1,h}=1} \mathrm{b}_h(\underline{\boldsymbol{v}}_h, q_h)}$$

- This stability result is valid on general meshes and for any $k \geq 0$

Convective term I

- Recall the skew-symmetric expression of t:

$$t(\boldsymbol{w}, \boldsymbol{u}, \boldsymbol{v}) = \frac{1}{2} \int_{\Omega} \boldsymbol{v}^{\mathrm{T}} \boldsymbol{\nabla} \boldsymbol{u}\, \boldsymbol{w} - \frac{1}{2} \int_{\Omega} \boldsymbol{u}^{\mathrm{T}} \boldsymbol{\nabla} \boldsymbol{v}\, \boldsymbol{w}$$

- Inspired by this reformulation, we set

$$\boxed{\mathrm{t}_h(\underline{\boldsymbol{w}}_h, \underline{\boldsymbol{u}}_h, \underline{\boldsymbol{v}}_h) \coloneqq \frac{1}{2} \int_{\Omega} \boldsymbol{v}_h^{\mathrm{T}} \boldsymbol{G}_h^{2k} \underline{\boldsymbol{u}}_h\, \boldsymbol{w}_h - \frac{1}{2} \int_{\Omega} \boldsymbol{u}_h^{\mathrm{T}} \boldsymbol{G}_h^{2k} \underline{\boldsymbol{v}}_h\, \boldsymbol{w}_h}$$

- By design, t_h is non dissipative: For all $\underline{\boldsymbol{w}}_h, \underline{\boldsymbol{v}}_h$,

$$\mathrm{t}_h(\underline{\boldsymbol{w}}_h, \underline{\boldsymbol{v}}_h, \underline{\boldsymbol{v}}_h) = 0$$

Convective term II

- In practice, one does not need to actually compute $\boldsymbol{G}_h^{2k}$
- In fact, expanding $\boldsymbol{G}_h^{2k}$ according to its definition, we have

$$\mathrm{t}_h(\underline{\boldsymbol{w}}_h, \underline{\boldsymbol{u}}_h, \underline{\boldsymbol{v}}_h) = \sum_{T \in \mathcal{T}_h} t_T(\underline{\boldsymbol{w}}_T, \underline{\boldsymbol{u}}_T, \underline{\boldsymbol{v}}_T),$$

where, for all $T \in \mathcal{T}_h$,

$$\begin{aligned} t_T(\underline{\boldsymbol{w}}_T, \underline{\boldsymbol{u}}_T, \underline{\boldsymbol{v}}_T) \coloneqq &-\frac{1}{2}\int_T \boldsymbol{u}_T^{\mathrm{T}} \boldsymbol{\nabla} \boldsymbol{v}_T\, \boldsymbol{w}_T + \frac{1}{2}\sum_{F \in \mathcal{F}_T} \int_F (\boldsymbol{u}_F \cdot \boldsymbol{v}_T)(\boldsymbol{w}_T \cdot \boldsymbol{n}_{TF}) \\ &+ \frac{1}{2}\int_T \boldsymbol{v}_T^{\mathrm{T}} \boldsymbol{\nabla} \boldsymbol{u}_T\, \boldsymbol{w}_T - \frac{1}{2}\sum_{F \in \mathcal{F}_T} \int_F (\boldsymbol{v}_F \cdot \boldsymbol{u}_T)(\boldsymbol{w}_T \cdot \boldsymbol{n}_{TF}) \end{aligned}$$

Discrete problem I

The discrete problem reads: Find $(\underline{\boldsymbol{u}}_h, p_h) \in \underline{\boldsymbol{U}}_{h,0}^k \times P_h^k$ s.t.

$$\boxed{\begin{aligned} \nu \mathrm{a}_h(\underline{\boldsymbol{u}}_h, \underline{\boldsymbol{v}}_h) + \mathrm{t}_h(\underline{\boldsymbol{u}}_h, \underline{\boldsymbol{u}}_h, \underline{\boldsymbol{v}}_h) + \mathrm{b}_h(\underline{\boldsymbol{v}}_h, p_h) &= \int_\Omega \boldsymbol{f} \cdot \boldsymbol{v}_h \quad && \forall \underline{\boldsymbol{v}}_h \in \underline{\boldsymbol{U}}_{h,0}^k, \\ -\mathrm{b}_h(\underline{\boldsymbol{u}}_h, q_h) &= 0 && \forall q_h \in P_h^k \end{aligned}}$$

Well-posedness I

Theorem (Existence and a priori bounds)

There exists a solution $(\underline{\boldsymbol{u}}_h, p_h) \in \underline{\boldsymbol{U}}_{h,0}^k \times P_h^k$ *such that*

$$\begin{aligned} \|\underline{\boldsymbol{u}}_h\|_{1,h} &\leq C_a C_s \nu^{-1} \|\boldsymbol{f}\|, \\ \|p_h\| &\leq C \left(\|\boldsymbol{f}\| + \nu^{-2}\|\boldsymbol{f}\|^2\right), \end{aligned}$$

with C_s *discrete Poincaré constant, and* $C > 0$ *independent of* h *and* ν*.*

Theorem (Uniqueness of the discrete solution)

Assume that the forcing term verifies

$$\|\boldsymbol{f}\| \leq \frac{\nu^2}{2C_a^2 C_t C_s}$$

with C_t *continuity constant of* t_h*. Then, the solution is unique.*

Convergence I

Theorem (Convergence to minimal regularity solutions)

It holds up to a subsequence, as $h \to 0$,

- $\boldsymbol{u}_h \to \boldsymbol{u}$ *strongly in* $L^p(\Omega)^d$ *for* $p \in [1, +\infty)$ *if* $d = 2$, $p \in [1, 6)$ *if* $d = 3$;
- $\boldsymbol{G}_h^k \underline{\boldsymbol{u}}_h \to \boldsymbol{\nabla u}$ *strongly in* $L^2(\Omega)^{d \times d}$;
- $\mathrm{s}_h(\underline{\boldsymbol{u}}_h, \underline{\boldsymbol{u}}_h) \to 0$;
- $p_h \to p$ *strongly in* $L^2(\Omega)$.

If the exact solution is unique, the whole sequence converges.

Key tools: discrete Sobolev embeddings and Rellick–Kondrachov compactness results from [DP and Droniou, 2017a]

Convergence II

Theorem (Convergence rates for small data)

Assume uniqueness for both $(\underline{\boldsymbol{u}}_h, p_h)$ *and* $(\boldsymbol{u}, p)$*. Assume, moreover, the additional regularity* $(\boldsymbol{u}, p) \in H^{k+2}(\Omega)^d \times H^{k+1}(\Omega)$*, as well as*

$$\|\boldsymbol{f}\| \leq \frac{\nu^2}{2C_I C_a C_t (1 + C_{\mathrm{P}}^2)},$$

with C_a *and* C_t *as above,* C_I *boundedness constant of* $\underline{\boldsymbol{I}}_h^k$*, and* C_{P} *continuous Poincaré constant. Then, with hidden constant independent of both* h *and* ν*,*

$$\|\underline{\boldsymbol{u}}_h - \underline{\boldsymbol{I}}_h^k \boldsymbol{u}\|_{1,h} + \nu^{-1}\|p_h - \pi_h^{0,k} p\|_{L^2(\Omega)} \lesssim h^{k+1} \mathcal{N}_{\boldsymbol{u},p}.$$

with $\mathcal{N}_{\boldsymbol{u},p} := (1 + \nu^{-1}\|\boldsymbol{u}\|_{H^2(\Omega)^d})\|\boldsymbol{u}\|_{H^{k+2}(\Omega)^d} + \nu^{-1}\|p\|_{H^{k+1}(\Omega)}$*,*

Static condensation

- Partition the discrete velocity unknowns as before, and the pressure unknowns into average value + oscillations inside each element
- At each iteration, the linear system has the form

$$\begin{bmatrix} \mathsf{A}_{\mathcal{T}_h\mathcal{T}_h} & \widetilde{\mathsf{B}}_{\mathcal{T}_h} & \mathsf{A}_{\mathcal{T}_h\mathcal{F}_h^{\mathrm{i}}} & \overline{\mathsf{B}}_{\mathcal{T}_h} \\ \mathsf{A}_{\mathcal{F}_h^{\mathrm{i}}\mathcal{T}_h} & \widetilde{\mathsf{B}}_{\mathcal{F}_h^{\mathrm{i}}} & \mathsf{A}_{\mathcal{F}_h^{\mathrm{i}}\mathcal{F}_h^{\mathrm{i}}} & \overline{\mathsf{B}}_{\mathcal{F}_h^{\mathrm{i}}} \\ \widetilde{\mathsf{B}}_{\mathcal{T}_h}^{\mathrm{T}} & 0 & \widetilde{\mathsf{B}}_{\mathcal{F}_h^{\mathrm{i}}}^{\mathrm{T}} & 0 \\ \overline{\mathsf{B}}_{\mathcal{T}_h}^{\mathrm{T}} & 0 & \overline{\mathsf{B}}_{\mathcal{F}_h^{\mathrm{i}}}^{\mathrm{T}} & 0 \end{bmatrix} \begin{bmatrix} \mathsf{U}_{\mathcal{T}_h} \\ \widetilde{\mathsf{P}}_{\mathcal{T}_h} \\ \mathsf{U}_{\mathcal{F}_h^{\mathrm{i}}} \\ \overline{\mathsf{P}}_{\mathcal{T}_h} \end{bmatrix} = \begin{bmatrix} \mathsf{F}_{\mathcal{T}_h} \\ 0 \\ 0 \\ 0 \end{bmatrix}$$

- Static condensation of $\mathsf{U}_{\mathcal{T}_h}$ and $\widetilde{\mathsf{P}}_{\mathcal{T}_h}$ is possible
- **Impact of static condensation on the global matrix?**

Numerical example: Kovasznay flow

- We consider the exact solution of [Kovasznay, 1948].
- Let $\Omega \coloneqq (-0.5, 1.5) \times (0, 2)$ and set

$$\mathrm{Re} \coloneqq (2\nu)^{-1}, \qquad \lambda \coloneqq \mathrm{Re} - \left(\mathrm{Re}^2 + 4\pi^2\right)^{\frac{1}{2}}$$

- The components of the velocity are given by

$$u_1(\boldsymbol{x}) \coloneqq 1 - \exp(\lambda x_1)\cos(2\pi x_2), \qquad u_2(\boldsymbol{x}) \coloneqq \frac{\lambda}{2\pi}\exp(\lambda x_1)\sin(2\pi x_2),$$

  and pressure given by

$$p(\boldsymbol{x}) \coloneqq -\frac{1}{2}\exp(2\lambda x_1) + \frac{\lambda}{2}\left(\exp(4\lambda) - 1\right)$$

Numerical example: Kovasznay flow

Cartesian mesh family, $\nu = 0.1$

h	$\\|\underline{\boldsymbol{u}}_h - \widehat{\underline{\boldsymbol{u}}}_h\\|_{1,h}$	OCR	$\\|\boldsymbol{u}_h - \widehat{\boldsymbol{u}}_h\\|$	OCR	$\\|p_h - \widehat{p}_h\\|$	OCR
			$k = 0$			
0.13	1.02	—	0.33	—	1.84	—
$6.25 \cdot 10^{-2}$	0.55	0.89	0.17	0.99	0.21	3.14
$3.12 \cdot 10^{-2}$	0.34	0.68	$4.31 \cdot 10^{-2}$	1.94	$4.36 \cdot 10^{-2}$	2.26
$1.56 \cdot 10^{-2}$	0.19	0.86	$1.09 \cdot 10^{-2}$	1.98	$1.37 \cdot 10^{-2}$	1.67
$7.81 \cdot 10^{-3}$	$9.72 \cdot 10^{-2}$	0.96	$2.7 \cdot 10^{-3}$	2.02	$3.78 \cdot 10^{-3}$	1.86
			$k = 1$			
0.13	0.45	—	0.15	—	0.44	—
$6.25 \cdot 10^{-2}$	0.24	0.94	$3.39 \cdot 10^{-2}$	2.11	$3.45 \cdot 10^{-2}$	3.68
$3.12 \cdot 10^{-2}$	$6.46 \cdot 10^{-2}$	1.86	$4.26 \cdot 10^{-3}$	2.99	$8.58 \cdot 10^{-3}$	2
$1.56 \cdot 10^{-2}$	$1.78 \cdot 10^{-2}$	1.86	$5.58 \cdot 10^{-4}$	2.93	$1.23 \cdot 10^{-3}$	2.8
$7.81 \cdot 10^{-3}$	$4.65 \cdot 10^{-3}$	1.94	$7.11 \cdot 10^{-5}$	2.98	$1.87 \cdot 10^{-4}$	2.72
			$k = 2$			
0.13	0.25	—	$6.41 \cdot 10^{-2}$	—	$9.8 \cdot 10^{-2}$	—
$6.25 \cdot 10^{-2}$	$4.83 \cdot 10^{-2}$	2.34	$5.81 \cdot 10^{-3}$	3.46	$7.55 \cdot 10^{-3}$	3.7
$3.12 \cdot 10^{-2}$	$7.11 \cdot 10^{-3}$	2.76	$3.45 \cdot 10^{-4}$	4.06	$7.71 \cdot 10^{-4}$	3.28
$1.56 \cdot 10^{-2}$	$1.01 \cdot 10^{-3}$	2.82	$2.07 \cdot 10^{-5}$	4.06	$7 \cdot 10^{-5}$	3.46
$7.81 \cdot 10^{-3}$	$1.34 \cdot 10^{-4}$	2.92	$1.25 \cdot 10^{-6}$	4.06	$6.54 \cdot 10^{-6}$	3.43
			$k = 3$			
0.13	$7.84 \cdot 10^{-2}$	—	$2.1 \cdot 10^{-2}$	—	$3.46 \cdot 10^{-2}$	—
$6.25 \cdot 10^{-2}$	$7.5 \cdot 10^{-3}$	3.39	$8.03 \cdot 10^{-4}$	4.71	$1.39 \cdot 10^{-3}$	4.64
$3.12 \cdot 10^{-2}$	$5.11 \cdot 10^{-4}$	3.87	$2.52 \cdot 10^{-5}$	4.98	$7.31 \cdot 10^{-5}$	4.24
$1.56 \cdot 10^{-2}$	$3.43 \cdot 10^{-5}$	3.9	$8.15 \cdot 10^{-7}$	4.95	$3.87 \cdot 10^{-6}$	4.24
$7.81 \cdot 10^{-3}$	$2.22 \cdot 10^{-6}$	3.96	$2.59 \cdot 10^{-8}$	4.98	$2.17 \cdot 10^{-7}$	4.16

Numerical example: Kovasznay flow

Hexagonal mesh family, $\nu = 0.1$

h	$\|\underline{\boldsymbol{u}}_h - \widehat{\underline{\boldsymbol{u}}}_h\|_{1,h}$	OCR	$\|\boldsymbol{u}_h - \widehat{\boldsymbol{u}}_h\|$	OCR	$\|p_h - \widehat{p}_h\|$	OCR
			$k = 0$			
0.14	1.64	—	0.62	—	2.1	—
$7.33 \cdot 10^{-2}$	0.64	1.44	0.19	1.81	0.24	3.31
$3.69 \cdot 10^{-2}$	0.44	0.56	$7.12 \cdot 10^{-2}$	1.42	$9.99 \cdot 10^{-2}$	1.28
$1.85 \cdot 10^{-2}$	0.25	0.79	$2.32 \cdot 10^{-2}$	1.62	$3.94 \cdot 10^{-2}$	1.35
$9.27 \cdot 10^{-3}$	0.13	0.91	$6.7 \cdot 10^{-3}$	1.8	$1.32 \cdot 10^{-2}$	1.58
			$k = 1$			
0.14	0.53	—	0.22	—	0.28	—
$7.33 \cdot 10^{-2}$	0.22	1.32	$3.95 \cdot 10^{-2}$	2.64	$5.25 \cdot 10^{-2}$	2.58
$3.69 \cdot 10^{-2}$	$7.26 \cdot 10^{-2}$	1.63	$4.81 \cdot 10^{-3}$	3.07	$1.26 \cdot 10^{-2}$	2.08
$1.85 \cdot 10^{-2}$	$1.96 \cdot 10^{-2}$	1.9	$5.81 \cdot 10^{-4}$	3.06	$2.37 \cdot 10^{-3}$	2.42
$9.27 \cdot 10^{-3}$	$5.07 \cdot 10^{-3}$	1.96	$6.75 \cdot 10^{-5}$	3.12	$4.07 \cdot 10^{-4}$	2.55
			$k = 2$			
0.14	0.28	—	$7.84 \cdot 10^{-2}$	—	0.11	—
$7.33 \cdot 10^{-2}$	$5.23 \cdot 10^{-2}$	2.56	$6.37 \cdot 10^{-3}$	3.84	$1.19 \cdot 10^{-2}$	3.39
$3.69 \cdot 10^{-2}$	$8.32 \cdot 10^{-3}$	2.68	$5.32 \cdot 10^{-4}$	3.62	$1.7 \cdot 10^{-3}$	2.84
$1.85 \cdot 10^{-2}$	$1.16 \cdot 10^{-3}$	2.85	$3.74 \cdot 10^{-5}$	3.85	$2.04 \cdot 10^{-4}$	3.07
$9.27 \cdot 10^{-3}$	$1.52 \cdot 10^{-4}$	2.94	$2.44 \cdot 10^{-6}$	3.95	$2.61 \cdot 10^{-5}$	2.98
			$k = 3$			
0.14	$7.1 \cdot 10^{-2}$	—	$1.56 \cdot 10^{-2}$	—	$2.23 \cdot 10^{-2}$	—
$7.33 \cdot 10^{-2}$	$9.66 \cdot 10^{-3}$	3.05	$1.1 \cdot 10^{-3}$	4.05	$2.31 \cdot 10^{-3}$	3.47
$3.69 \cdot 10^{-2}$	$8.97 \cdot 10^{-4}$	3.46	$5.36 \cdot 10^{-5}$	4.4	$1.7 \cdot 10^{-4}$	3.8
$1.85 \cdot 10^{-2}$	$6.8 \cdot 10^{-5}$	3.74	$2.13 \cdot 10^{-6}$	4.67	$1.08 \cdot 10^{-5}$	3.99
$9.27 \cdot 10^{-3}$	$4.68 \cdot 10^{-6}$	3.87	$7.6 \cdot 10^{-8}$	4.82	$6.69 \cdot 10^{-7}$	4.03

Numerical example: Kovasznay flow

Hexagonal mesh family, HDG trilinear form, $\nu = 0.1$

h	$\Vert\underline{\boldsymbol{u}}_h - \widehat{\underline{\boldsymbol{u}}}_h\Vert_{1,h}$	OCR	$\Vert\boldsymbol{u}_h - \widehat{\boldsymbol{u}}_h\Vert$	OCR	$\Vert p_h - \widehat{p}_h\Vert$	OCR
			$k = 1$			
0.14			Not converged			
$7.33 \cdot 10^{-2}$	0.22	—	$3.99 \cdot 10^{-2}$	—	$4.83 \cdot 10^{-2}$	—
$3.69 \cdot 10^{-2}$	$7.01 \cdot 10^{-2}$	1.65	$4.94 \cdot 10^{-3}$	3.04	$9.91 \cdot 10^{-3}$	2.31
$1.85 \cdot 10^{-2}$	$1.94 \cdot 10^{-2}$	1.86	$5.87 \cdot 10^{-4}$	3.09	$1.94 \cdot 10^{-3}$	2.36
$9.27 \cdot 10^{-3}$	$5.04 \cdot 10^{-3}$	1.95	$6.64 \cdot 10^{-5}$	3.15	$3.5 \cdot 10^{-4}$	2.48
			$k = 2$			
0.14			Not converged			
$7.33 \cdot 10^{-2}$	$4.96 \cdot 10^{-2}$	—	$6.36 \cdot 10^{-3}$	—	$9.52 \cdot 10^{-3}$	—
$3.69 \cdot 10^{-2}$	$8.38 \cdot 10^{-3}$	2.59	$5.52 \cdot 10^{-4}$	3.56	$1.38 \cdot 10^{-3}$	2.81
$1.85 \cdot 10^{-2}$	$1.18 \cdot 10^{-3}$	2.84	$3.92 \cdot 10^{-5}$	3.83	$1.73 \cdot 10^{-4}$	3.01
$9.27 \cdot 10^{-3}$	$1.55 \cdot 10^{-4}$	2.94	$2.58 \cdot 10^{-6}$	3.94	$2.25 \cdot 10^{-5}$	2.95
			$k = 3$			
0.14	$6.69 \cdot 10^{-2}$	—	$1.52 \cdot 10^{-2}$	—	$1.65 \cdot 10^{-2}$	—
$7.33 \cdot 10^{-2}$	$9.61 \cdot 10^{-3}$	2.97	$1.1 \cdot 10^{-3}$	4.01	$1.91 \cdot 10^{-3}$	3.3
$3.69 \cdot 10^{-2}$	$9.14 \cdot 10^{-4}$	3.43	$5.56 \cdot 10^{-5}$	4.35	$1.5 \cdot 10^{-4}$	3.71
$1.85 \cdot 10^{-2}$	$6.99 \cdot 10^{-5}$	3.72	$2.24 \cdot 10^{-6}$	4.65	$9.86 \cdot 10^{-6}$	3.94
$9.27 \cdot 10^{-3}$	$4.83 \cdot 10^{-6}$	3.87	$8.01 \cdot 10^{-8}$	4.82	$6.17 \cdot 10^{-7}$	4.01

References I

Aghili, J., Boyaval, S., and Di Pietro, D. A. (2015).
Hybridization of mixed high-order methods on general meshes and application to the Stokes equations.
Comput. Meth. Appl. Math., 15(2):111–134.

Aghili, J. and Di Pietro, D. A. (2017).
An advection-robust Hybrid High-Order method for the Oseen problem.
Preprint hal-01541389.

Botti, L., Di Pietro, D. A., and Droniou, J. (2018).
A robust Hybrid High-Order discretisation of the Brinkman problem.
Submitted.

Di Pietro, D. A. and Droniou, J. (2017a).
A Hybrid High-Order method for Leray–Lions elliptic equations on general meshes.
Math. Comp., 86(307):2159–2191.

Di Pietro, D. A. and Droniou, J. (2017b).
$W^{s,p}$-approximation properties of elliptic projectors on polynomial spaces, with application to the error analysis of a Hybrid High-Order discretisation of Leray–Lions problems.
Math. Models Methods Appl. Sci., 27(5):879–908.

Di Pietro, D. A. and Ern, A. (2015).
A hybrid high-order locking-free method for linear elasticity on general meshes.
Comput. Methods Appl. Mech. Engrg., 283:1–21.

Di Pietro, D. A., Ern, A., and Lemaire, S. (2014).
An arbitrary-order and compact-stencil discretization of diffusion on general meshes based on local reconstruction operators.
Comput. Methods Appl. Math., 14(4):461–472.

Di Pietro, D. A., Ern, A., Linke, A., and Schieweck, F. (2016).
A discontinuous skeletal method for the viscosity-dependent Stokes problem.
Comput. Meth. Appl. Mech. Engrg., 306:175–195.

References II

Di Pietro, D. A. and Krell, S. (2017).
A Hybrid High-Order method for the steady incompressible Navier–Stokes problem.
J. Sci. Comput.
Published online. DOI 10.1007/s10915-017-0512-x.

Di Pietro, D. A. and Specogna, R. (2016).
An a posteriori-driven adaptive Mixed High-Order method with application to electrostatics.
J. Comput. Phys., 326(1):35–55.

Di Pietro, D. A. and Tittarelli, R. (2017).
An introduction to Hybrid High-Order methods.
Preprint arXiv:1703.05136.

Kovasznay, L. S. G. (1948).
Laminar flow behind a two-dimensional grid.
Proc. Camb. Philos. Soc., 44:58–62.